

# The Concealed Voter Model is in the Voter Model universality class

Rosalba Garcia-Millan<sup>1, 2, \*</sup>

<sup>1</sup>Department of Mathematics, Imperial College London, London SW7 2AZ, United Kingdom

<sup>2</sup>Centre for Complexity Science, Imperial College London, London SW7 2AZ, UK

(Dated: 21st December 2024)

The Concealed Voter Model (CVM) is an extension of the original Voter Model, where two different opinions compete until consensus is reached. In the CVM, agents express an opinion not only publicly, they also hold a private opinion, which they may disclose or change. In this paper I derive the critical exponents of both models via renormalised field theory and show that both belong to the compact directed percolation universality class.

## I. INTRODUCTION

The Concealed Voter Model (CVM) is a simple agent-based model of opinion formation in social networks that takes into account the consistency or the lack thereof between a voter's private and publicly expressed opinions [1, 2]. In the original Voter Model (VM), agents adopt the expressed opinion of one of their neighbours at random until the system reaches consensus [3]. Modelling the private opinion of agents in the CVM is introduced as an extension to the VM in [1].

The VM is a special case of the Domany-Kinzel cellular automaton, which is in the universality class of compact directed percolation, also known as the VM universality class [4–6]. To determine whether the CVM belongs to the same universality class, I calculate the critical exponents characterising the spreading of an opinion from a localised source via a path integral approach. In [7], a path-integral method was used to compute the persistence probability on a slight variation of the VM.

In the VM, each agent expresses one of two opinions, which may be thought of as particles and empty sites on a  $d$ -dimensional lattice, Fig. 1. At rate  $\alpha > 0$ , every agent **copies** the opinion expressed by one of their randomly chosen neighbours. The system is initialised with a single particle, and the process of copying is repeated until the system reaches one of the two absorbing states: all sites either empty or occupied. In the VM, activity only happens at the boundaries between clusters of empty and occupied sites. The critical point of the VM separates the two phases where, in the thermodynamic limit, particles are subject to extinction with probability 1 and where there is a positive probability of indefinite survival. Microscopically, the VM is at criticality if given

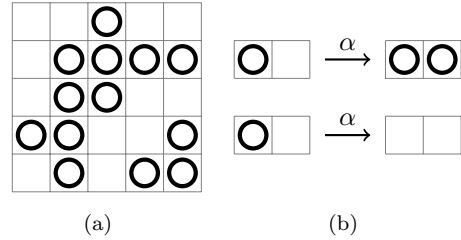


**Figure 1:** The voter model (opinions are represented by circles and empty spaces). (a) Sample of a particle configuration in the VM in  $d = 2$ . (b) The process of copying at the cluster boundary.

a pair of neighbours at the interface between clusters  $(1, 0)$ , the two possible outcomes after copying,  $(0, 0)$  and  $(1, 1)$ , are equally likely. If, for instance, the former is more likely, then, on average, there is a net loss of particles that gives rise to the mass in the field theory. The VM at criticality is also known as unbiased voter [5] and it is representative of so-called neutral theories [8].

Observables commonly considered to characterise such critical processes are [9, 10]: the expected number of particles  $n(t)$  at time  $t$ , the mean square spread of particles  $R^2(t)$  (or radius of gyration), and the survival probability  $P_s(t)$ , namely, the probability that there is at least one particle in the system. At criticality, these three observables have an asymptotic algebraic scaling in time,

$$\langle n(t) \rangle \propto t^\eta, \quad R^2(t) \propto t^z, \quad P_s(t) \propto t^{-\delta}, \quad (1)$$

whose exponents  $\eta$ ,  $z$  and  $\delta$  characterise the VM universality class. Due to the duality between the VM and coalescent random walks [5, 6, 10], it is known that  $\eta = 0$  and  $z = 1$ , and  $\delta = 1/2$  at dimension  $d = 1$  and  $\delta = 1$  for dimensions  $d \geq 2$ , satisfying the hyperscaling relation [5]

$$\delta + \eta = \frac{1}{2} dz \quad (2)$$

\* garciamillan16@imperial.ac.uk

in dimensions  $d \leq 2$ .

In Sec. II, I derive the field theory of the VM and calculate the critical exponents; in Sec. III, I incorporate the dynamics of the CVM in the field theory and calculate the critical exponents. Finally, I discuss the results in Sec. IV.

## II. CRITICAL EXPONENTS OF THE VOTER MODEL

The critical exponents of the VM are well understood [5, 10]. Nevertheless, in this section, the exponents of the VM are derived via a path integral approach to lay the foundations of the derivation of the critical exponents of the CVM in Sec. III.

The configuration of the system is given by the set  $\{\mathbf{m}\}$  of occupation numbers  $m_x$ , which is the number of particles at lattice site  $x$ . The dynamics of the VM are condensed in the following master equation,

$$\begin{aligned} \dot{P}(\{\mathbf{m}\}; t) = & \sum_{x,y} \left\{ \alpha (m_x + 1) \left(1 - \frac{m_y}{c}\right) P(m_x + 1, m_y; t) \right. \\ & + \alpha m_y \left(1 - \frac{m_x - 1}{c}\right) P(m_x - 1, m_y; t) \\ & \left. - \alpha \left[ m_x \left(1 - \frac{m_y}{c}\right) + m_y \left(1 - \frac{m_x}{c}\right) \right] P(m_x, m_y; t) \right\}, \end{aligned}$$

where  $P(\{\mathbf{m}\}; t)$  is the probability of finding the system in microstate  $\{\mathbf{m}\}$  at time  $t$ ,  $x$  and  $y$  are nearest neighbours, and  $c$  is the carrying capacity, the maximum number of particles allowed in each site. This carrying capacity implements the fermionic nature of opinions and may be set to  $c = 1$ . However, it is useful to parametrise this excluded volume constraint as it is the only interaction that keeps the spreading of particles at bay [11–13]. The first term in Eq. (3) describes the elimination of a particle at  $x$  by an empty space at  $y$ , the second, the production of a particle at  $x$  by a particle at  $y$ . Initially, at time  $t_0 = 0$ , a single particle is placed at  $\mathbf{x}_0$ . Following the Doi-Peliti formalism, the master equation in (3) is cast in path integral form [14]. After taking the continuum limit and introducing the annihilation field  $\phi(\mathbf{x}, t)$  and the Doi-shifted creation field  $\tilde{\phi}(\mathbf{x}, t)$ , the action functional of the resulting field theory is  $\mathcal{A}_0 + \mathcal{A}_{\text{int}}$ , where

$$\mathcal{A}_0 = \int d^d x dt \left\{ \tilde{\phi} \partial_t \phi - D \tilde{\phi} \nabla^2 \phi + r \tilde{\phi} \phi \right\}, \quad (4)$$

and

$$\begin{aligned} \mathcal{A}_{\text{int}} = & \int d^d x dt \left\{ -s \tilde{\phi}^2 \phi + \chi \tilde{\phi}^2 \phi^2 \right. \\ & \left. + w_1 \tilde{\phi} (\nabla^2 \phi) \tilde{\phi} - w_2 \tilde{\phi} (\nabla^2 \phi) \tilde{\phi}^2 \phi + w_3 \tilde{\phi}^3 \phi^2 \right\}, \end{aligned} \quad (5)$$

$D = \alpha$  is the effective diffusion constant,  $s = \alpha d$  is the effective branching rate, and the other non-linearities are  $\chi = \alpha d/c$ ,  $w_1 = \alpha$ ,  $w_2 = \alpha/c$  and  $w_3 = \alpha d$ . The mass  $r > 0$  of the particles is added to regularise the infrared, ensuring causality in the time domain  $t \geq t_0$ , and is later removed by taking the limit  $r \rightarrow 0$  at criticality. The action functional allows the calculation of an observable  $\mathcal{O}$ , via the path integral

$$\langle \mathcal{O} \rangle = \int \mathcal{D}[\phi, \tilde{\phi}] \mathcal{O} e^{-(\mathcal{A}_0 + \mathcal{A}_{\text{int}})}, \quad (6)$$

which satisfies the normalisation condition  $\langle 1 \rangle = 1$ .

In the VM, it is expected that the long range behaviour in time and space is governed by the processes of effective diffusion and effective branching. For this reason, it can be assumed that  $D$  and  $s$  have independent dimensions,  $[D] = B$  and  $[s] = A$ . Along with  $[x] = L$  and the dimensionlessness of the action functional,  $[\mathcal{A}_0 + \mathcal{A}_{\text{int}}] = 1$ , it follows that

$$\begin{aligned} (3) \quad [\phi] = L^{-d+2} AB^{-1}, \quad [\tilde{\phi}] = L^{-2} A^{-1} B, \quad (7) \\ [t] = L^2 B^{-1}, \quad [r] = L^{-2} B, \quad [\chi] = L^{d-2} B, \\ [w_1] = L^2 A, \quad [w_2] = L^{d+2} A, \quad [w_3] = L^d A, \end{aligned}$$

implying that the couplings  $w_1$ ,  $w_2$  and  $w_3$  are irrelevant, which yields the action functional in (4) and (5) consistent with [5, 10]. The coupling  $\chi$  has critical dimension  $d_c = 2$  such that  $\chi$  is relevant for  $d < d_c$ , marginal at  $d = d_c$  and irrelevant for  $d > d_c$ . The fact that, in terms of the original parameters, the coupling  $\chi$  is inversely proportional to the carrying capacity  $c$  indicates that  $\chi$  arises from the excluded-volume interactions between particles, which, according to the critical dimension  $d_c$  become irrelevant for dimensions  $d > d_c$ .

The Fourier transform is defined, by convention, as

$$\phi(\mathbf{k}, \omega) = \int d^d x dt e^{i\omega t - i\mathbf{k} \cdot \mathbf{x}} \phi(\mathbf{x}, t), \quad (8a)$$

$$\phi(\mathbf{x}, t) = \int d^d \mathbf{k} d\omega e^{-i\omega t + i\mathbf{k} \cdot \mathbf{x}} \phi(\mathbf{k}, \omega), \quad (8b)$$

where the spatial momentum  $\mathbf{k}$  is conjugate of the position  $\mathbf{x}$ , the frequency  $\omega$  is conjugate of time  $t$ ,  $d^d \mathbf{k} = d^d \mathbf{k} / (2\pi)^d$  and  $d\omega = d\omega / 2\pi$ .

The same convention applies to  $\tilde{\phi}(t)$ . It is often convenient to use Feynman diagrams to express lengthy expressions [14]. In the diagrams, time, or the direction of causality as implemented by the positive mass  $r$ , is read from right to left. The bare propagator of the  $\phi$  field is then, from Eq. (4),

$$\begin{aligned} \phi \quad \tilde{\phi} &\doteq \left\langle \phi(\mathbf{k}, \omega) \tilde{\phi}(\mathbf{k}', \omega') \right\rangle \quad (9) \\ &= \frac{\delta(\omega + \omega') \delta(\mathbf{k} + \mathbf{k}')}{-i\omega + D\mathbf{k}^2 + r}. \end{aligned}$$

### A. Exponents $\eta$ and $z$

The expected number of particles in the system is

$$n(t) = \int d^d \mathbf{x} \left\langle \phi(\mathbf{x}, t) \tilde{\phi}(\mathbf{x}_0, t_0) \right\rangle = e^{-rt}, \quad (10)$$

for  $r > 0$ . At criticality,  $r = 0$ , the expected number of particles is  $n(t) = 1$ , so that  $\eta = 0$  according to Eq. (1). The mean square spread of particles is

$$\begin{aligned} R^2(t) &= \int d^d \mathbf{x} (\mathbf{x} - \mathbf{x}_0)^2 \left\langle \phi(\mathbf{x}, t) \tilde{\phi}(\mathbf{x}_0, t_0) \right\rangle \\ &= -\frac{d^2}{d\mathbf{k}^2} \left( \int d\omega e^{-i\omega t} \left\langle \phi(\mathbf{k}, \omega) \tilde{\phi}(\mathbf{k}', \omega') \right\rangle \right) \Big|_{\mathbf{k}=0} \\ &= 2Dte^{-rt} \end{aligned} \quad (11)$$

for  $r > 0$ , and, at the critical point,  $R^2(t) \propto t$ , so that  $z = 1$ . The reason why both exponents,  $\eta$  and  $z$ , attain their trivial values is the non-renormalisation of the propagator.

### B. Exponent $\delta$

According to [15], the survival probability is given by

$$P_s(r, D, s, \chi; t) = - \left\langle e^{-\int d^d \mathbf{x} \phi(\mathbf{x}, t) \tilde{\phi}(\mathbf{x}_0, t_0)} \right\rangle \quad (12a)$$

$$= - \sum_{n=0}^{\infty} \frac{(-1)^n}{n!} \left\langle \left( \int d^d \mathbf{x} \phi(\mathbf{x}, t) \right)^n \tilde{\phi}(\mathbf{x}_0, t_0) \right\rangle \quad (12b)$$

$$\doteq - \sum_{n=0}^{\infty} \frac{(-1)^n}{n!} \quad n \left\{ \begin{array}{c} \vdots \\ \text{hatched circle} \end{array} \right\} \quad (12c)$$

where the hatched circle in Eq. (12c) indicates the sum over all diagrams that have one incoming leg and  $n$  outgoing legs. For instance, the

two tree-level contributions to  $n = 4$  are

$$\begin{array}{c} \text{Diagram 1} \\ \text{Diagram 2} \end{array} \quad (13)$$

At tree level, the sum (12c) is easily performed to produce

$$P_s(r, D, s, \chi; t) = \frac{\exp(-rt)}{1 + \frac{s}{r} (1 - \exp(-rt))}, \quad (14)$$

which becomes

$$P_s(0, D, s, \chi; t) = \frac{1}{1 + st} \quad (15)$$

in the limit of  $r \rightarrow 0$ . However, in  $d < 2$ , where  $\chi$  is relevant, loop diagrams contribute to the survival probability, whose effect is captured by replacing the bare  $s$  in (14) by an effective (renormalised) coupling. This non-linearity renormalises under dimensional regularisation at  $d = 2 - \epsilon$ , by means of the governing non-linearity  $\chi$ , which renormalises itself.

The effective, renormalised, couplings  $\chi_{\text{eff}}$  and  $s_{\text{eff}}$  are, diagrammatically,

$$\chi_{\text{eff}} = \chi + \chi \text{ loop } \chi + \chi \text{ loop } \chi + \dots \quad (16a)$$

$$s_{\text{eff}} = s + \chi \text{ loop } s + \chi \text{ loop } \chi \text{ loop } s + \dots \quad (16b)$$

which can be summed exactly,

$$\chi_{\text{eff}} = \frac{\chi}{1 + \mathcal{J}\chi}, \quad (17a)$$

$$s_{\text{eff}} = \frac{s}{1 + \mathcal{J}\chi}, \quad (17b)$$

taking into account that  $s$  enters in the expansion of the exponential of the action in Eq. (6) with a positive sign and  $\chi$  with a negative sign, and where  $\mathcal{J}$  is the loop integral

$$\mathcal{J} = \text{hatched circle} \quad (18a)$$

$$\begin{aligned} &\doteq \int d^d \mathbf{k}_1 d^d \mathbf{k}_2 d^d \mathbf{k}_3 d^d \mathbf{k}_4 d\omega_1 d\omega_2 d\omega_3 d\omega_4 \\ &\quad \times \delta(\mathbf{k}_2 + \mathbf{k}_4) \delta(\mathbf{k}_1 + \mathbf{k}_3) \delta(\omega_2 + \omega_4) \delta(\omega_1 + \omega_3) \\ &\quad \times \left\langle \phi(\mathbf{k}_2, \omega_2) \tilde{\phi}(\mathbf{k}_1, \omega_1) \right\rangle \left\langle \phi(\mathbf{k}_4, \omega_4) \tilde{\phi}(\mathbf{k}_3, \omega_3) \right\rangle \\ &= \frac{r^{\frac{d}{2}-1}}{(4\pi D)^{\frac{d}{2}}} \Gamma\left(1 - \frac{d}{2}\right) \simeq \frac{2r^{-\frac{\epsilon}{2}}}{\epsilon(4\pi D)^{\frac{d}{2}}}, \end{aligned} \quad (18b)$$

with  $d = 2 - \epsilon$ .

Defining the  $Z$ -factors such that  $\chi_{\text{eff}} = \chi Z_\chi$  and  $s_{\text{eff}} = s Z_s$ , from Eq. (17) it follows that the two  $Z$ -factors are equal,  $Z_\chi = Z_s$ , yielding the renormalisation of the coupling  $s$  entirely driven by the renormalisation of  $\chi$ . It is noteworthy that the renormalisation of this pair of couplings satisfies the Ward identity [12]

$$\frac{\chi_{\text{eff}}}{\chi} = \frac{ds_{\text{eff}}}{ds}. \quad (19)$$

The renormalisation of the dimensionless coupling  $\chi_{\mathcal{R}} = \mu^{-\epsilon} \mathcal{U} \chi_{\text{eff}}$ , where  $\mu = \sqrt{r/D}$  is an arbitrary inverse length scale and  $\mathcal{U} = 2/(D(4\pi)^{d/2})$ , is, using Eqs. (17), (18) and the identity  $x = y/(1+ay) = y(1-ax)$ , exactly

$$\chi_{\mathcal{R}} = \mu^{-\epsilon} \mathcal{U} \chi \left(1 - \frac{1}{\epsilon} \chi_{\mathcal{R}}\right). \quad (20)$$

The  $\beta$ -function of the renormalised governing coupling  $\chi_{\mathcal{R}}$  is

$$\beta_\chi = \mu \frac{d}{d\mu} \chi_{\mathcal{R}} = -\epsilon \chi_{\mathcal{R}} + \chi_{\mathcal{R}}^2, \quad (21)$$

whose infrared-stable fixed point is  $\chi_{\mathcal{R}}^* = \epsilon$  since  $d\beta_\chi(\chi_{\mathcal{R}}^* = \epsilon)/d\chi_{\mathcal{R}} = \epsilon > 0$ . Since both  $Z$ -factors are identical,  $Z_\chi = Z_s = 1 - \chi_{\mathcal{R}}/\epsilon$ , the Wilson  $\gamma$ -functions of the couplings are then identical as well,

$$\gamma_s = \gamma_\chi = \mu \frac{d}{d\mu} \log Z_\chi = \frac{-1}{\epsilon Z_\chi} \beta_\chi = \chi_{\mathcal{R}} \rightarrow \chi_{\mathcal{R}}^*. \quad (22)$$

Then, the anomalous dimensions of  $s$  and  $\chi$  are  $\gamma_s = \gamma_\chi = \epsilon$  for  $\epsilon > 0$ . For  $\epsilon < 0$ , the infrared-stable fixed point of  $\beta_\chi$  is  $\chi^* = 0$  as  $d\beta_\chi(\chi^* = 0)/d\chi_{\mathcal{R}} = -\epsilon > 0$ , and therefore  $\gamma_s = \gamma_\chi = 0$ . As a result, in dimensions  $d > 2$  the anomalous dimensions of  $s$  and  $\chi$  vanishes and the process exhibits mean-field behaviour as correlations due to volume exclusion become irrelevant.

Dimensional consistency in Eq. (14) requires  $[s] = [r]$  and therefore  $A = L^{-2}B$ . As  $[P_s] = 1$  it follows that

$$\begin{aligned} P_s(r, D, s, \chi; t) & \quad (23) \\ & = P_s \left( \frac{r}{L^{-2}B}, \frac{D}{B}, \frac{s}{L^{-2}B}, \frac{\chi}{L^{-\epsilon}B}; \frac{t}{L^2B^{-1}} \right), \end{aligned}$$

for any positive, real  $L, B$ . A similar expression can be found for all vertex functions. Following the usual process [14] of using (23) with  $B = D$  and  $L = \sqrt{Dt}$  in conjunction with the solution of the Callan Symanzik equation on the basis

of the Wilson  $\gamma$ -functions (22) produces

$$P_s(r, D, s, \chi; t) = P_s \left( rt, 1, st\ell^{\gamma_s}, \frac{\chi \ell^{\gamma_\chi}}{D(Dt)^{-\epsilon/2}}; 1 \right), \quad (24)$$

with a dimensionless, small scale parameter  $\ell$ , which one may choose to be  $\ell = (D/\chi \cdot (Dt)^{-\epsilon/2})^{1/\gamma_\chi}$ , such that at  $\epsilon > 0$ , when  $\gamma_s = \gamma_\chi = \epsilon$ ,

$$P_s(r, D, s, \chi; t) = P_s \left( rt, 1, \frac{s}{\chi} (Dt)^{1-\frac{\epsilon}{2}}, 1; 1 \right). \quad (25)$$

As the accounts for the effect of the interaction that takes hold at large times by adjusting parameters in an expression involving (arbitrarily) short times, when the tree-level theory applies, the survival probability at criticality is expected to be (15)

$$P_s(0, D, s, \chi; t) = \frac{1}{1 + \frac{s}{\chi} (Dt)^{1-\frac{\epsilon}{2}}}. \quad (26)$$

Asymptotically in  $t$ ,

$$P_s(0, D, s, \chi; t) \propto t^{-(1-\frac{\epsilon}{2})}, \quad (27)$$

which implies by Eq. (1) that  $\delta = 1 - \epsilon/2$  for  $d < 2$ . For  $d \geq 2$  the  $\gamma$ -functions vanish so that  $\delta = 1$ , with logarithmic corrections at  $d = d_c = 2$ , recovering the results in [5].

### III. CRITICAL EXPONENTS OF THE CONCEALED VOTER MODEL

In addition to the lattice (outer layer) of the voter model above, where opinions are copied to nearest neighbours with rate  $\alpha$ , the CVM has an inner layer, that represents the private opinion of each agent, which may equal or differ from the expressed opinion in the outer layer, Fig. 2. The private and publicly expressed opinions interact via two new processes: an agent may **externalise** their private opinion with rate  $\beta$  (the opinion in the inner layer is copied into the outer layer) and **internalise** their expressed opinion with rate  $\gamma$  (the opinion in the outer layer is copied into the inner layer). In total, there are three concurrent Poisson processes: copying at rate  $\alpha$ , externalisation at rate  $\beta$  and internalisation at rate  $\gamma$ . The original VM is recovered if  $\beta = 0$  [1].

As in the VM, the interaction between two competing opinions can be represented by the interactions between particles and empty spaces. The particles in the two layers may be considered two distinct species, namely, mobile

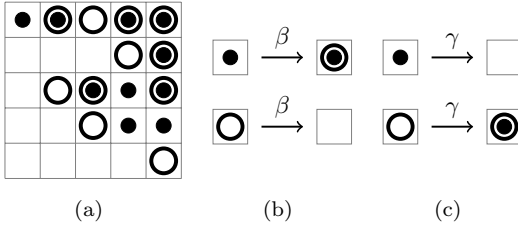


**Figure 2:** The concealed voter model (opinions in the outer layer are represented by circles and empty spaces, and, in the inner layer, by solid disks and empty spaces). (a) Sample of a particle configuration in the CVM in  $d = 2$ . (b) Externalisation process between the two layers. (c) Internalisation process between the two layers. The process of copying in the outer layer is represented in Fig. 1(b).

particles with occupation numbers  $\{m\}$  and immobile particles with occupation numbers  $\{n\}$  [11, 12].

The master equation of the CVM comprises in addition to Eq. (3) for the process of copy-

ing (the left-hand side of the equation becomes  $\dot{P}_\alpha(\{m\}; t)$ ) the following contribution

$$\begin{aligned} \dot{P}_\beta(\{m\}, \{n\}; t) = & \sum_x \left\{ \beta(m_x + 1) \left(1 - \frac{n_x}{c}\right) P(n_x, m_x + 1; t) \right. \\ & + \beta n_x \left(1 - \frac{m_x - 1}{c}\right) P(n_x, m_x - 1; t) \\ & \left. - \beta \left[m_x \left(1 - \frac{n_x}{c}\right) + n_x \left(1 - \frac{m_x}{c}\right)\right] P(n_x, m_x; t) \right\}, \end{aligned} \quad (28)$$

for the process of externalisation with rate  $\beta$ , and a symmetric transformation of the above for the process of internalisation obtained by swapping  $m_x$  for  $n_x$ , the rate  $\beta$  for  $\gamma$ . Hence, the time evolution of the microstate probability is  $\dot{P}(\{m\}, \{n\}; t) = \dot{P}_\alpha(\{m\}; t) + \dot{P}_\beta(\{m\}, \{n\}; t) + \dot{P}_\gamma(\{m\}, \{n\}; t)$ . At time  $t_0 = 0$ , the system is initialised with one particle of either species with equal probability at  $\mathbf{x}_0$ .

It follows that the action functional  $\mathcal{A}'_0 + \mathcal{A}'_{\text{int}}$  of the CVM is

$$\mathcal{A}'_0 = \int d^d x dt \left\{ \tilde{\phi} \partial_t \phi - D \tilde{\phi} \nabla^2 \phi + r_1 \tilde{\phi} \phi + \tilde{\psi} \partial_t \psi + r_2 \tilde{\psi} \psi - \tau_1 \psi \tilde{\phi} - \tau_2 \phi \tilde{\psi} \right\} \quad (29a)$$

$$\begin{aligned} \mathcal{A}'_{\text{int}} = & \int d^d x dt \left\{ -s \tilde{\phi}^2 \phi - \sigma_1 \tilde{\psi} \psi \tilde{\phi} - \sigma_2 \tilde{\phi} \phi \tilde{\psi} + \chi \tilde{\phi}^2 \phi^2 + \kappa_1 \psi \tilde{\phi}^2 \phi + \kappa_2 \phi \tilde{\psi}^2 \psi \right. \\ & \left. + w_1 \tilde{\phi} (\nabla^2 \phi) \tilde{\phi} - w_2 \tilde{\phi} (\nabla^2 \phi) \tilde{\phi}^2 \phi + w_3 \tilde{\phi}^3 \phi^2 + w_4 \tilde{\psi} \psi \tilde{\phi}^2 \phi + w_5 \tilde{\phi} \phi \tilde{\psi}^2 \psi \right\} \end{aligned} \quad (29b)$$

where  $\psi$  is the annihilation and  $\tilde{\psi}$  is the Doi-shifted creation field of the immobile species, and where, in terms of the model parameters,  $r_1 = \tau_1 = \sigma_1 = \beta$  (associated with externalisation),  $r_2 = \tau_2 = \sigma_2 = \gamma$  (associated with internalisation),  $\kappa_1 = w_4 = \beta/c$  and  $\kappa_2 = w_5 = \gamma/c$ . The couplings  $\tau_1$  and  $\tau_2$  are commonly referred to as transmutations [11, 12], as they provide causal correlations between fields of different species. This terminology may lead to confusion though, if one thinks of particles in one species changing into the other species. In the CVM it is more accurate to say that immobile particles deposit mobile particles with rate  $\beta$  and mobile particles deposit immobile particles with rate  $\gamma$ . Assuming that  $L$ ,  $A$  and  $B$  are independent dimensions, and that the two fields  $\phi$  and  $\psi$  have the same dimensions,  $[\phi] = [\psi] = L^{-d+2}AB^{-1}$ , the dimensions of the

new couplings are

$$\begin{aligned} [r_1] &= [r_2] = [\tau_1] = [\tau_2] = BL^{-2}, \quad (30) \\ [\sigma_1] &= [\sigma_2] = A, [\kappa_1] = [\kappa_2] = L^{d-2}B, \\ [w_4] &= [w_5] = L^d A. \end{aligned}$$

This implies that  $w_4$  and  $w_5$  are irrelevant nonlinearities, while all the others are either relevant or marginal.

The couplings  $s$  and  $\chi$  stay as in the VM, but the new couplings  $\sigma_1$ ,  $\sigma_2$ ,  $\kappa_1$  and  $\kappa_2$  couple the new  $\psi$ ,  $\tilde{\psi}$  fields to the old  $\phi$ ,  $\tilde{\phi}$ . Diagrammatically,

$$\text{---}^{\sigma_1}, \text{---}^{\sigma_2}, \text{---}^{\kappa_1}, \text{---}^{\kappa_2}, \quad (31)$$

where  represents the propagator  $\langle \psi \tilde{\psi} \rangle$ . This set of mixed couplings encode correlations between the two species due to transmutation and volume exclusion. From Eq. (29a), the four response propagators  $\langle \phi \tilde{\phi} \rangle$ ,  $\langle \psi \tilde{\psi} \rangle$ ,  $\langle \phi \tilde{\psi} \rangle$  and

$\langle \psi \tilde{\phi} \rangle$  are determined, App. A.

In fact, all six  $s$ -like couplings (one incoming leg and two outgoing legs) are effectively available by combining  $s$ ,  $\sigma_1$  or  $\sigma_2$  with suitable propagators, and are denoted by  $\sigma_3, \dots, \sigma_5$ . Similarly, the nine  $\chi$ -like couplings (two incoming and two outgoing legs) are available, by combining  $\chi$ ,  $\kappa_1$  or  $\kappa_2$  with the propagators, and are denoted by  $\kappa_3, \dots, \kappa_8$ . Therefore, the one-loop renormalisation of each of the available couplings may need to consider sixteen loop integrals, which are reduced to ten integrals due to their symmetries, App. B.

However, to define the observables  $n(t)$ ,  $R^2(t)$  and  $P_s(t)$  in the CVM, it is convenient to consider the total number of particles, irrespectively of their species. Indeed, the system will reach an absorbing state whenever the total population is zero. This motivates the definition of the annihilation *density* field  $\rho = \phi + \psi$  (and the Doi-shifted creation density field  $\tilde{\rho} = \tilde{\phi} + \tilde{\psi}$ ), whose propagator is, using the propagators in App. A,

$$\begin{aligned} \rho \text{---} \tilde{\rho} &\hat{=} \langle \rho(\mathbf{k}, \omega) \tilde{\rho}(\mathbf{k}', \omega') \rangle \quad (32) \\ &= \delta(\omega + \omega') \delta(\mathbf{k} + \mathbf{k}') \\ &\times \frac{-2i\omega + D\mathbf{k}^2 + r_1 + r_2 + \tau_1 + \tau_2}{(-i\omega + D\mathbf{k}^2 + r_1)(-i\omega + r_2) - \tau_1 \tau_2}. \end{aligned}$$

The critical point of the CVM happens when particles, *i.e.* one of the two opinions, are no longer subject to *spontaneous* extinction,  $r_1 = \tau_1$  and  $r_2 = \tau_2$ . That is, when the gain and loss of particles due to deposition and decay are balanced: immobile particles through the internalisation process, and mobile particles through the externalisation process. To deal with the infrared divergence at criticality, it can be assumed that  $r_1 = \tau_1 + r$  and  $r_2 = \tau_2 + r$ , taking the limit  $r \rightarrow 0$  to reach the critical point.

The loop integrals in App. B contain two infrared divergencies,  $r \rightarrow 0$  and  $\tau_1 + \tau_2 \rightarrow 0$ , where the second one corresponds to the original VM at criticality. Henceforth, I assume  $\tau_1 + \tau_2 > 0$  and refer to  $r \rightarrow 0$  as the critical point of the CVM. Moreover, the loop integral  $I_{10}$  in Eq. (B11) has a quadratic divergence that results from taking the continuum limit. Since the process is originally defined on the lattice, this divergence can be regularised by introducing an ultraviolet cutoff.

### A. Exponents $\eta$ and $z$

The expected number of particles is

$$n(t) = \frac{1}{2} \int d^d \mathbf{x} \langle \rho(\mathbf{x}, t) \tilde{\rho}(\mathbf{x}_0, t_0) \rangle = e^{-rt}, \quad (33)$$

where the factor of 1/2 accounts for a particle of either species being created with equal probability. At  $r = 0$ , *i.e.* at the critical point  $n(t) = 1$ , and the critical exponent in Eq. (1) is  $\eta = 0$ . The mean square spread of mobile particles is

$$\begin{aligned} R^2(t) &= \frac{1}{2} \int d^d \mathbf{x} (\mathbf{x} - \mathbf{x}_0)^2 \langle \rho(\mathbf{x}, t) \tilde{\rho}(\mathbf{x}_0, t_0) \rangle \quad (34) \\ &= \frac{dD}{\tau_1 + \tau_2} e^{-rt} \left[ 2\tau_2 t + \frac{\tau_1 - \tau_2}{\tau_1 + \tau_2} \left( 1 - e^{-(\tau_1 + \tau_2)t} \right) \right]. \end{aligned}$$

At the critical point  $R^2(t) \propto t$ , so the critical exponent is  $z = 1$ .

Eq. (34) recovers the behaviour of the original voter model, Eq. (11), for vanishing transmutation, depending on how this limit is taken. For  $\tau_1 = 0$ ,  $\tau_2 \rightarrow 0$  and  $\tau_2 = 0$ ,  $\tau_1 \rightarrow 0$  the mean square spread is half of that of Eq. (11), as the spread is zero if the initial particle happens to be immobile.

### B. Exponent $\delta$

The survival probability in the CVM is

$$\begin{aligned} P_s(r, \tau_1, \tau_2, D, s, \sigma_1, \dots, \sigma_5, \chi, \kappa_1, \dots, \kappa_8; t) \\ = -\frac{1}{2} \left\langle e^{-\int d^d \mathbf{x} \rho(\mathbf{x}, t) \tilde{\rho}(\mathbf{x}_0, t_0)} \right\rangle \quad (35a) \end{aligned}$$

$$= -\frac{1}{2} \sum_{n=0}^{\infty} \frac{(-1)^n}{n!} \left\langle \left( \int d^d \mathbf{x} \rho(\mathbf{x}, t) \right)^n \tilde{\rho}(\mathbf{x}_0, t_0) \right\rangle$$

$$\hat{=} -\frac{1}{2} \sum_{n=0}^{\infty} \frac{(-1)^n}{n!} \quad n \left\{ \begin{array}{c} \text{---} \\ \vdots \\ \text{---} \end{array} \right\} \quad (35b)$$

where the sum contains all binary tree diagrams with one incoming  $\tilde{\rho}$  field and  $n$  outgoing  $\rho$  fields.

To account for the transmutations between the  $\phi$  and  $\psi$  fields in the sum in Eq. (35), the density field  $\rho$  alone is not enough. To make use of the symmetries that will later allow for simplifications, I consider the *polarity* fields  $\nu = \phi - \psi$  and  $\tilde{\nu} = (\tau_1 \tilde{\phi} - \tau_2 \tilde{\psi})/(\tau_1 + \tau_2)$ . The fields  $\phi$ ,  $\tilde{\phi}$ ,  $\psi$ ,  $\tilde{\psi}$  are then mapped to the fields  $\rho$ ,  $\tilde{\rho}$ ,  $\nu$ ,  $\tilde{\nu}$ , by means of linear combinations. The propagators  $\langle \nu \tilde{\nu} \rangle$ ,  $\langle \rho \tilde{\rho} \rangle$  and  $\langle \nu \tilde{\rho} \rangle$  are stated explicitly in App. C. Similarly, the couplings involving  $\rho$ ,  $\tilde{\rho}$ ,  $\nu$ ,  $\tilde{\nu}$ , are weighted lin-

ear combinations of  $s, \sigma_1, \dots, \sigma_5, \chi, \kappa_1, \dots, \kappa_8$  and all observables may be parametrised in terms of these linear combinations weighted by powers of  $\tau_1/(\tau_1 + \tau_2)$  and  $\tau_2/(\tau_1 + \tau_2)$  as they enter  $\tilde{v}$ . Eq. (35) is thus simply a reparametrisation of the survival probability in terms of linear combinations of couplings. Consider, for example, the branching non-linearity involving only  $\rho$  and  $\tilde{\rho}$  fields

$$\text{Diagram with label } \zeta \text{ (36)}$$

with  $\zeta = \tau_2(s\tau_2 + \tau_1(\sigma_1 + \sigma_2))/(2(\tau_1 + \tau_2)^2)$ , and the four-legged non-linearity involving only  $\rho$  and  $\tilde{\rho}$  fields

$$\text{Diagram with label } \lambda \text{ (37)}$$

with  $\lambda = (\tau_2^2(\chi + \kappa_1) + \tau_1^2\kappa_2)/(4(\tau_1 + \tau_2)^2)$ .

For example, for  $n = 3$ , the sum in Eq. (35) has contributions from diagrams such as

$$\text{Diagrams with labels } \zeta, \zeta, \lambda, \text{ (38)}$$

where  represents the propagator  $\langle v \tilde{v} \rangle$ .

In what follows I show that any addend in Eq. (35) containing a  $v$  or a  $\tilde{v}$  field is asymptotically sub-leading and, therefore, its contribution can be neglected. From the propagators in App. C, it follows that the propagators in real time, integrated over all space, are

$$\int d^d x \langle v(x, t) \tilde{v}(x_0, t_0) \rangle = -e^{-(\tau_1 + \tau_2 + r)t}, \quad (39a)$$

$$\int d^d x \langle \rho(x, t) \tilde{\rho}(x_0, t_0) \rangle = \frac{\tau_2 - \tau_1}{\tau_1 + \tau_2} e^{-(\tau_1 + \tau_2 + r)t}, \quad (39b)$$

$$\int d^d x \langle v(x, t) \tilde{\rho}(x_0, t_0) \rangle = 0, \quad (39c)$$

which decay exponentially faster in time  $t$  than  $\int d^d x \langle \rho(x, t) \tilde{\rho}(x_0, t_0) \rangle = 2e^{-rt}$  in Eq. (33), since  $r \rightarrow 0$  while  $\tau_1, \tau_2 > 0$ . Hence, only binary tree diagrams containing  $\rho$  and  $\tilde{\rho}$  asymptotically contribute to the sum in Eq. (35), which gives

$$P_s(r, \tau_1, \tau_2, D, s, \sigma_1, \dots, \sigma_5, \chi, \kappa_1, \dots, \kappa_8; t) \simeq \frac{\exp(-rt)}{2 \left( 1 + \frac{\zeta}{r} (1 - \exp(-rt)) \right)}. \quad (40)$$

Further, the fields  $v$  and  $\tilde{v}$  are also present in

the renormalisation of the non-linearities. For example,  $\zeta$  is renormalised diagrammatically by,

$$\text{Diagram with label } \zeta_R = \text{Diagram with label } \zeta + \lambda \text{ (41)}$$

and similarly for the four-legged diagrams, which are, in fact, the governing non-linearities. However, it can be shown that any loops containing  $v$  or  $\tilde{v}$  are ultraviolet convergent as far as the phase transition at  $r \rightarrow 0$  is concerned. Expressing the loops formed with  $\rho, \tilde{\rho}, v, \tilde{v}$  as linear combinations of the loops formed with  $\phi, \tilde{\phi}, \psi, \tilde{\psi}$  in Sec. B, and assuming  $\tau_1 + \tau_2 > 0$ , it follows that the only ultraviolet divergence to be taken into account is

$$\mathcal{K} = \text{Diagram with label } \lambda \text{ (42a)}$$

$$\begin{aligned} & \hat{=} \int d^d k_1 d^d k_2 d^d k_3 d^d k_4 d\omega_1 d\omega_2 d\omega_3 d\omega_4 \\ & \times \delta(\mathbf{k}_2 + \mathbf{k}_4) \delta(\mathbf{k}_1 + \mathbf{k}_3) \delta(\omega_2 + \omega_4) \delta(\omega_1 + \omega_3) \\ & \times \langle \rho(\mathbf{k}_2, \omega_2) \tilde{\rho}(\mathbf{k}_1, \omega_1) \rangle \langle \rho(\mathbf{k}_4, \omega_4) \tilde{\rho}(\mathbf{k}_3, \omega_3) \rangle \\ & = 2 \left( \frac{\tau_1 + \tau_2}{\tau_2 4\pi D} \right)^{\frac{d}{2}} r^{\frac{d}{2}-1} \Gamma \left( 1 - \frac{d}{2} \right), \end{aligned} \quad (42b)$$

whereas all the other loop integrals are ultraviolet convergent,

$$\begin{aligned} 0 & \hat{=} \text{Diagram with label } \zeta = \text{Diagram with label } \lambda = \text{Diagram with label } \zeta = \text{Diagram with label } \lambda \\ & = \text{Diagram with label } \zeta = \text{Diagram with label } \lambda = \text{Diagram with label } \zeta = \text{Diagram with label } \lambda. \end{aligned} \quad (43)$$

In conclusion, the renormalisation of the reparametrised non-linearities is solely run by  $\lambda$ , in the same way that, in the VM,  $\chi$  is the governing non-linearity. It follows that the arguments in Sec. II B for the VM apply equally to the CVM, producing the same result for the critical exponent  $\delta$  in the CVM as in the VM.

## IV. DISCUSSION AND CONCLUSIONS

In summary, the CVM has the same asymptotic behaviour as the VM at criticality and, therefore, the CVM belongs to the VM universality class. The addition of the inner layer and the new interactions with the external layer introduce changes in the short-term dynamics of the process, where the inner layer acts as an internal memory of previous states. However, the

new interactions are not strong enough to significantly change the long-range and long-term behaviour of the process.

Yet, the interactions in the CVM manage to cause havoc to the renormalisation calculation and require linear combinations of fields and couplings to be considered. The field theory encounters a range of interesting technical challenges. For example, since the VM at criticality is a particular case of the CVM, the loop integrals involved in the CVM present multiple infrared divergencies. Moreover, the renormalisation of the field theory in  $\phi$  and  $\psi$  involves ten loop integrals for a set of fifteen coupled nonlinearities. Nevertheless, the renormalisation scheme greatly simplifies by reparametrising the non-linearities by suitable linear transformations of the fields that make use of the intrinsic symmetries of the field theory of the CVM.

## ACKNOWLEDGMENTS

I am indebted to Gunnar Pruessner, who has taught me almost all I know about field theory. I would also like to thank Luca Cocconi, Miguel Muñoz, Mauro Mobilia, Michael Gastner and the Non-Equilibrium Systems group at Imperial College for useful discussions.

## Appendix A: Propagators involving $\phi$ and $\psi$

From Eq. (29a), the four response propagators  $\langle \phi \tilde{\phi} \rangle$ ,  $\langle \psi \tilde{\psi} \rangle$ ,  $\langle \phi \tilde{\psi} \rangle$ ,  $\langle \psi \tilde{\phi} \rangle$ , are read off from the inverse of the bilinear interaction matrix as follows:

$$\begin{aligned} \phi \underline{\tilde{\phi}} &= \underline{\text{---}} + \underline{\text{---}} + \underline{\text{---}} + \dots \\ &\hat{=} \langle \phi(\mathbf{k}, \omega) \tilde{\phi}(\mathbf{k}', \omega') \rangle \\ &= \frac{\delta(\omega + \omega') \delta(\mathbf{k} + \mathbf{k}') (-i\omega + r_2)}{(-i\omega + D\mathbf{k}^2 + r_1) (-i\omega + r_2) - \tau_1 \tau_2}, \end{aligned} \quad (\text{A1})$$

$$\begin{aligned} \psi \underline{\tilde{\psi}} &= \underline{\text{---}} + \underline{\text{---}} + \underline{\text{---}} + \dots \\ &\hat{=} \langle \psi(\mathbf{k}, \omega) \tilde{\psi}(\mathbf{k}', \omega') \rangle \\ &= \frac{\delta(\omega + \omega') \delta(\mathbf{k} + \mathbf{k}') (-i\omega + D\mathbf{k}^2 + r_1)}{(-i\omega + D\mathbf{k}^2 + r_1) (-i\omega + r_2) - \tau_1 \tau_2}, \end{aligned} \quad (\text{A2})$$

$$\begin{aligned} \phi \underline{\tilde{\psi}} &= \underline{\text{---}} + \underline{\text{---}} + \dots \\ &\hat{=} \langle \phi(\mathbf{k}, \omega) \tilde{\psi}(\mathbf{k}', \omega') \rangle \end{aligned} \quad (\text{A3})$$

$$= \frac{\delta(\omega + \omega') \delta(\mathbf{k} + \mathbf{k}') \tau_1}{(-i\omega + D\mathbf{k}^2 + r_1) (-i\omega + r_2) - \tau_1 \tau_2},$$

$$\begin{aligned} \psi \underline{\tilde{\phi}} &= \underline{\text{---}} + \underline{\text{---}} + \dots \\ &\hat{=} \langle \psi(\mathbf{k}, \omega) \tilde{\phi}(\mathbf{k}', \omega') \rangle \end{aligned} \quad (\text{A4})$$

$$= \frac{\delta(\omega + \omega') \delta(\mathbf{k} + \mathbf{k}') \tau_2}{(-i\omega + D\mathbf{k}^2 + r_1) (-i\omega + r_2) - \tau_1 \tau_2}.$$

## Appendix B: Loop integrals with $\phi$ and $\psi$

Let  $r_i = \tau_i + r$ ,  $i \in \{1, 2\}$ , in Eq. (A1)–(A4) and

$$\tilde{U} = \frac{(\tau_1 + \tau_2)^{\frac{d}{2}-2}}{2\tau_2(4\pi D)^{d/2}} \Gamma\left(1 - \frac{d}{2}\right), \quad (\text{B1})$$

then the loop integrals involving the fields  $\phi$ ,  $\tilde{\phi}$ ,  $\psi$ ,  $\tilde{\psi}$ , are

$$I_1 = \text{---} \hat{=} \tilde{U} \left( \tau_1 \tau_2 + \tau_2^2 \left( \frac{r}{\tau_2} \right)^{\frac{d}{2}-1} \right), \quad (\text{B2})$$

$$I_2 = \text{---} \hat{=} \tilde{U} \left( -\tau_1 \tau_2 + \tau_1 \tau_2 \left( \frac{r}{\tau_2} \right)^{\frac{d}{2}-1} \right), \quad (\text{B3})$$

$$I_3 = \text{---} \hat{=} \tilde{U} \left( -\tau_2^2 + \tau_2^2 \left( \frac{r}{\tau_2} \right)^{\frac{d}{2}-1} \right), \quad (\text{B4})$$

$$I_4 = \text{---} \hat{=} \tilde{U} \left( \tau_1 \tau_2 + 2\tau_2^2 + \tau_1 \tau_2 \left( \frac{r}{\tau_2} \right)^{\frac{d}{2}-1} \right), \quad (\text{B5})$$

$$I_5 = \text{---} \hat{=} \tilde{U} \left( -\tau_1^2 + \tau_1^2 \left( \frac{r}{\tau_2} \right)^{\frac{d}{2}-1} \right), \quad (\text{B6})$$

$$I_6 = \text{---} \hat{=} I_2, \quad (\text{B7})$$

$$I_7 = \text{---} \hat{=} I_3, \quad (\text{B8})$$

$$I_8 = \text{Diagram} \hat{=} \tilde{U} \left( \tau_2^2 + \tau_1 \tau_2 \left( \frac{r}{\tau_2} \right)^{\frac{d}{2}-1} \right), \quad (\text{B9})$$

$$I_9 = \text{Diagram} \hat{=} \tilde{U} \left( \tau_1 \tau_2 + \tau_1^2 \left( \frac{r}{\tau_2} \right)^{\frac{d}{2}-1} \right), \quad (\text{B10})$$

$$I_{10} = \text{Diagram} \hat{=} \frac{\Lambda^d}{2\tau_2} + I_9, \quad (\text{B11})$$

where  $\Lambda < \infty$  is an ultraviolet cutoff to regularise the quadratic divergence of  $I_{10}$  at  $d = d_c$  as  $\mathbf{k} \rightarrow \infty$ . The loop  $I_{10}$  is UV finite with a quadratic divergence entering only as the internal layer becomes inert in the absence of internalisation,  $\tau_2 \rightarrow 0$ . All loops above have the same divergence as  $r \rightarrow 0$ , the critical point of the CVM, up to an amplitude in powers of  $\tau_1$  and  $\tau_2$  that is effectively accounted for by the linear combination of fields introduced with  $\tilde{v}$ . In any loops that contain  $v$  and  $\tilde{v}$  fields, which are constructed by subtracting fields  $\phi$ ,  $\psi$  and  $\tilde{\phi}$ ,  $\tilde{\psi}$  respectively, UV divergencies will therefore by symmetry vanish.

### Appendix C: Propagators involving $\rho$ and $v$

The propagators  $\langle v \tilde{v} \rangle$ ,  $\langle \rho \tilde{v} \rangle$ ,  $\langle v \tilde{\rho} \rangle$ , are

$$\begin{aligned} v_{\text{---} \bullet \bullet \bullet \bullet \bullet} \tilde{v} &\hat{=} \langle v(\mathbf{k}, \omega) \tilde{v}(\mathbf{k}', \omega') \rangle \\ &= \frac{\delta(\omega + \omega') \delta(\mathbf{k} + \mathbf{k}')}{\tau_1 + \tau_2} \\ &\times \frac{(\tau_1 + \tau_2)(-\imath\omega) + \tau_2 D\mathbf{k}^2 + \tau_1 r_2 + \tau_2 r_1 - 2\tau_1 \tau_2}{(-\imath\omega + D\mathbf{k}^2 + r_1)(-\imath\omega + r_2) - \tau_1 \tau_2}, \end{aligned} \quad (\text{C1})$$

$$\begin{aligned} \rho_{\text{---} \bullet \bullet \bullet \bullet} \tilde{v} &\hat{=} \langle \rho(\mathbf{k}, \omega) \tilde{v}(\mathbf{k}', \omega') \rangle \\ &= \frac{\delta(\omega + \omega') \delta(\mathbf{k} + \mathbf{k}')}{\tau_1 + \tau_2} \\ &\times \frac{(\tau_1 - \tau_2)(-\imath\omega) - \tau_2 D\mathbf{k}^2 + \tau_1 r_2 - \tau_2 r_1}{(-\imath\omega + D\mathbf{k}^2 + r_1)(-\imath\omega + r_2) - \tau_1 \tau_2}, \end{aligned} \quad (\text{C2})$$

$$\begin{aligned} v_{\text{---} \bullet \bullet \bullet \bullet} \tilde{\rho} &\hat{=} \langle v(\mathbf{k}, \omega) \tilde{\rho}(\mathbf{k}', \omega') \rangle \\ &= \delta(\omega + \omega') \delta(\mathbf{k} + \mathbf{k}') \\ &\times \frac{-D\mathbf{k}^2 + r_2 - r_1 + \tau_1 - \tau_2}{(-\imath\omega + D\mathbf{k}^2 + r_1)(-\imath\omega + r_2) - \tau_1 \tau_2}. \end{aligned} \quad (\text{C3})$$

---

[1] M. T. Gastner, B. Oborny, and M. Gulyás, *J. Stat. Mech.* **2018**, 063401 (2018).

[2] M. T. Gastner, K. Takács, M. Gulyás, Z. Szvetelszky, and B. Oborny, *PloS one* **14**, e0218729 (2019).

[3] T. M. Liggett, *Interacting Particle Systems* (Springer-Verlag, New York, NY, USA, 1985).

[4] E. Domany and W. Kinzel, *Phys. Rev. Lett.* **53**, 311 (1984).

[5] R. Dickman and A. Y. Tretyakov, *Phys. Rev. E* **52**, 3218 (1995).

[6] I. Dornic, H. Chaté, J. Chave, and H. A. Hinrichsen, *Phys. Rev. Lett.* **87**, 045701 (2001).

[7] M. Howard and C. Godreche, *J. Phys. A: Math. Gen.* **31**, L209 (1998).

[8] M. Martinello, J. Hidalgo, A. Maritan, S. Di Santo, D. Plenz, and M. A. Muñoz, *Phys. Rev. X* **7**, 041071 (2017).

[9] P. Grassberger and A. de la Torre, *Ann. Phys.* **122**, 373 (1979).

[10] M. A. Muñoz, Grinstein, and Y. Tu, *Phys. Rev. E* **56**, 5101 (1997).

[11] S. Nekovar and G. Pruessner, *J. Stat. Phys.* **163**, 604 (2016).

[12] I. Bordeu, S. Amarteifio, R. Garcia-Millan, B. Walter, N. Wei, and G. Pruessner, arXiv preprint arXiv:1909.00471 (2019).

[13] F. v. Wijland, *Phys. Rev. E* **63**, 022101 (2001).

[14] U. C. Täuber, *Critical dynamics* (Cambridge University Press, Cambridge, UK, 2014) pp. i–xvi, 1–511.

[15] R. Garcia-Millan, J. Pausch, B. Walter, and G. Pruessner, *Phys. Rev. E* **98**, 062107 (2018).